Nonlinear Science and Intelligent Applications
https://www.acadlore.com/journals/NSIA

Constraint-Induced Nonlinear Operating Regimes in Model Predictive Control: System-Level Dynamic Behaviour in Quadrotor Trajectory Tracking

Mohammed Mansour*, Mustafa Kutlu

Mechatronics Engineering Department, Sakarya Applied Sciences University, 54050 Serdivan, Turkey

* Correspondence: Mohammed Mansour (mohammedmansour@subu.edu.tr)

Received: 08-20-2025 **Revised:** 10-18-2025 **Accepted:** 10-30-2025

Citation: M. Mansour and M. Kutlu, "Constraint-induced nonlinear operating regimes in model predictive control: System-level dynamic behaviour in quadrotor trajectory tracking," *Nonlinear Sci. Intell. Appl.*, vol. 1, no. 2, pp. 65–73, 2025. https://doi.org/10.56578/nsia010202.

Abstract: Nonlinear dynamical systems operating under explicit constraints may exhibit qualitatively different closed-loop behaviours depending on the interaction between system coupling, feasibility boundaries, and feedback decision mechanisms. In constrained optimization-based control frameworks, such behaviour often manifests as distinct operating regimes and regime transitions that cannot be captured through local linear analysis. This study investigates constraint-induced nonlinear operating regimes arising in nonlinear model predictive control by considering quadrotor trajectory tracking as a representative constrained intelligent dynamical system. A physics-based rigid-body Newton–Euler model is embedded within a receding-horizon optimization framework with explicit actuator saturation and attitude safety constraints. Beyond conventional tracking objectives, the analysis adopts a system-level perspective to examine how nonlinear translational–rotational coupling and constraint activation jointly shape the qualitative structure of the closed-loop response. Comparative numerical simulations are conducted for both mild and aggressive reference maneuvers under varying constraint boundaries. The resulting responses reveal two dominant classes of nonlinear behaviour: constraint-inactive regimes, in which coupling-driven dynamics govern convergence characteristics, and constraint-active regimes, in which feasibility limits reallocate control authority and dominate transient response. Increased maneuver aggressiveness amplifies coupling-dominated effects, whereas tightened constraints induce regime transitions characterised by feasibility-driven dynamics. The results demonstrate that nonlinear model predictive control functions not only as an effective control strategy for constrained trajectory tracking, but also as a structured analytical tool for characterising regime-dependent behaviour in nonlinear intelligent systems. The findings provide insight into performance limitations, stability-relevant behaviour, and design trade-offs arising from the interplay between nonlinear dynamics and constraint geometry.

Keywords: Nonlinear model predictive control; Constraint-induced nonlinear regimes; Nonlinear dynamical behaviour; System-level analysis; Intelligent dynamical systems

1 Introduction

Quadrotor unmanned aerial vehicles have attracted substantial attention due to their mechanical simplicity, agility, and suitability for tasks ranging from inspection and surveillance to aerial manipulation and autonomous navigation [1]. Despite these advantages, quadrotor flight control remains fundamentally challenging because the system is inherently nonlinear, underactuated, and strongly coupled; translational accelerations are produced indirectly through attitude modulation, while rotational dynamics evolve under nonlinear rigid body interactions and bounded actuator authority [2]. Consequently, the closed-loop behavior of a quadrotor cannot be fully understood through linearized analysis around a single operating point, particularly when the vehicle executes time-varying trajectories or approaches feasibility limits. Traditional proportional–integral–derivative and linear-state feedback approaches can achieve stabilization near equilibrium, but their performance and interpretability degrade under constraints, aggressive maneuvers, or significant disturbances [3, 4].

From a nonlinear systems perspective, trajectory tracking is not merely a question of minimizing error; rather, it emerges from the interaction of nonlinear plant coupling, constraint boundaries that define feasible motion and actuation, and feedback decision mechanisms that compute control actions. This motivates the use of model predictive

control, which integrates prediction, optimization, and explicit constraint handling into a single framework [5, 6]. Nonlinear model predictive control extends classical model predictive control by employing nonlinear models within the receding-horizon optimization, making it particularly suitable for quadrotors [7, 8]. Importantly, nonlinear model predictive control can also serve as a structured tool for studying regime-dependent nonlinear behavior, since constraint activation can reshape the optimization solution and induce transitions between constraint-inactive and constraint-active operating regimes [9].

The application of nonlinear model predictive control to quadrotor unmanned aerial vehicle trajectory tracking has received considerable attention. Pereira et al. [10] formulated nonlinear model predictive control on SE(3) for aggressive tracking with state and input constraints and obstacle avoidance. Subsequent studies have addressed computational efficiency and stability-related properties for real-time flight, including contraction-based nonlinear model predictive control formulations and hierarchical architectures for robust navigation [11, 12]. Enhanced prediction fidelity has also been studied through learning-based and physics-based modeling refinements [13, 14]. In parallel, robustness to wind and uncertainty has been investigated using model predictive control variants such as localizer performance with vertical guidance-based formulations and robust decoupling strategies [15, 16]. Although these works have demonstrated the versatility of nonlinear model predictive control across scenarios, including payload suppression and recovery, constraints are frequently treated as performance enablers rather than as a driver of qualitative nonlinear regime behavior [17, 18]. Motivated by this gap, the present study reframes quadrotor nonlinear model predictive control tracking as an investigation of nonlinear closed-loop behavior shaped by constrained optimization. The manuscript is guided by the following scientific questions: How do nonlinear dynamics and explicit constraints jointly shape the transient and steady-state response? Do actuator and attitude limits induce distinct nonlinear regimes and transitions? How does the coupling between nonlinear prediction and constrained receding-horizon optimization influences stability-relevant behavior such as boundedness and smoothness? These questions shift the narrative from performance display alone to a system-level interpretation of constraint-induced dynamics.

To address these questions, this study develops a nonlinear model predictive control framework for quadrotor tracking using a continuous-time rigid-body model and constrained optimization. Simulation studies evaluate time-domain tracking, control input structure, and constraint-activation indicators under mild and aggressive maneuvers and under different constraint boundaries. The results enable both performance evaluation and regime-based interpretation of nonlinear closed-loop behavior.

2 Methodology

This section describes the nonlinear model predictive control framework and establishes the methodological elements required for system-level analysis of nonlinear closed loop behavior. Rather than treating the controller solely as a tracking mechanism, the proposed methodology is structured to expose how nonlinear translational rotational coupling, constraint boundaries, and receding-horizon optimization jointly shape the observed closed-loop regimes. The overall architecture (Figure 1) consists of a reference generator, a nonlinear prediction model, a constrained optimizer, and the quadrotor plant connected through state feedback. At each sampling instant, nonlinear model predictive control computes a control action by solving a nonlinear constrained optimal control problem using a physics-based rigid-body model and applying the first element of the optimal sequence according to the receding-horizon principle [6, 9, 19]. In addition to conventional tracking variables, the implementation logs constraint-activation indicators (thrust saturation, torque saturation, and attitude-bound proximity) to identify constraint-inactive and constraint-active operating regimes, enabling a regime-based interpretation consistent with hybrid and piecewise smooth viewpoints [20–22].

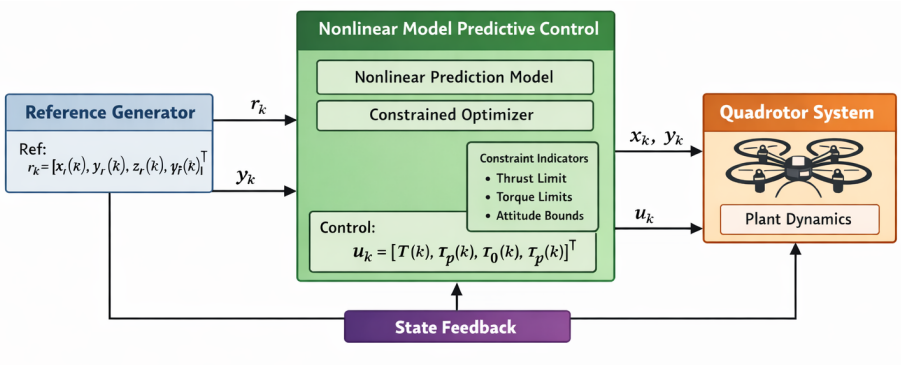

Figure 1. Block diagram of the proposed nonlinear model predictive control framework for quadrotor trajectory tracking

The block diagram in Figure 1 summarizes the signal flow. The reference generator provides desired outputs in Eq. (1), which are compared against the measured/estimated outputs, as shown in Eq. (2).

$$r_k = \begin{bmatrix} x_r(k) & y_r(k) & z_r(k) & \psi_r(k) \end{bmatrix}^\top \tag{1}$$

$$y_k = h(x_k) = \begin{bmatrix} p_x(k) & p_y(k) & p_z(k) & \psi(k) \end{bmatrix}^\top \tag{2}$$

The nonlinear model predictive control module uses the nonlinear prediction model and constraints to compute the manipulated variables as follows:

$$u_k = \begin{bmatrix} T(k) & \tau_\phi(k) & \tau_\theta(k) & \tau_\psi(k) \end{bmatrix}^\top \tag{3}$$

The resulting control inputs are applied to the plant dynamics. This closed-loop structure allows direct study of how reference excitation and feasibility boundaries influence control allocation, constraint engagement, and resultant nonlinear behavior. The quadrotor is modeled as a rigid body using continuous-time Newton–Euler dynamics. The state vector is as follows:

$$x = \begin{bmatrix} p_x & p_y & p_z & v_x & v_y & v_z & \phi & \theta & \psi & p \\ q & r & & & & & & & & \end{bmatrix}^\top \tag{4}$$

where, p_x, p_y, and p_z denote inertial positions, v_x, v_y, and v_z denote linear velocities, ϕ, θ, and ψ are roll–pitch–yaw angles (ZYX convention), and p, q, and r are body angular rates. The control input is as follows:

$$u = \begin{bmatrix} T & \tau_\phi & \tau_\theta & \tau_\psi \end{bmatrix}^\top \tag{5}$$

where, T is the total thrust and τ_ϕ, τ_θ, and τ_ψ are body torques.

2.1 Translational Dynamics

Let $R(\phi, \theta, \psi) \in R^{3\times 3}$ be the body-to-inertial rotation matrix. The translational dynamics are as follows:

$$\begin{aligned} \dot{p} &= v \\ \dot{v} &= \frac{1}{m} R(\phi, \theta, \psi) \begin{bmatrix} 0 \\ 0 \\ T \end{bmatrix} - \begin{bmatrix} 0 \\ 0 \\ g \end{bmatrix} \end{aligned} \tag{6}$$

Eq. (6) explicitly captures nonlinear coupling: horizontal accelerations require tilt (roll/pitch), which changes the thrust vector direction and introduces coupled effects between translation and attitude.

2.2 Rotational Dynamics

Let $\omega = [p\ q\ r]^\top$ and $\tau = [\tau_\phi\ \tau_\theta\ \tau_\psi]^\top$. The rotational dynamics are as follows:

$$\dot{\omega} = I^{-1} \left(\tau - \omega \times (I\omega) \right) \tag{7}$$

where, $I = \mathrm{diag}(I_x, I_y, I_z)$ is the inertia matrix. The Euler-angle kinematics are as follows:

$$\begin{aligned} \dot{\eta} &= E(\phi, \theta)\, \omega \\ \eta &= [\phi\ \theta\ \psi]^\top \end{aligned} \tag{8}$$

where, $E(\phi, \theta)$ denotes the standard ZYX mapping from body rates to Euler-angle rates. Eqs. (6)–(8) define the nonlinear prediction model used in nonlinear model predictive control.

At each sampling instant k, nonlinear model predictive control solves a finite-horizon constrained optimal control problem. The prediction model is as follows:

$$\begin{aligned} \dot{x}(t) &= f(x(t), u(t), p) \\ y(t) &= h(x(t)) \end{aligned} \tag{9}$$

where, p denotes the physical parameters. Using a sampling time T_s, the controller optimizes a sequence of manipulated variables over a prediction horizon N_p and applies the first action over $[kT_s, (k+1)T_s]$ [6, 9].

The objective penalizes tracking error, control effort, and control-rate variation:

$$J = \sum_{i=0}^{N_p-1} \left(\|y_{k+i} - r_{k+i}\|_Q^2 + \|u_{k+i}\|_R^2 + \|u_{k+i} - u_{k+i-1}\|_S^2 \right) \tag{10}$$

where, Q shapes the relative importance of tracking channels (vertical vs. horizontal); R regularizes control magnitudes; and S enforces smooth actuation by penalizing rate changes. Importantly, these parameters are not only performance knobs; they also influence regime boundaries by affecting how aggressively the optimizer drives the system toward constraint limits. This provides a methodological basis for analyzing how tuning choices reshape nonlinear closed-loop behavior [5].

The optimization is performed under explicit actuator and attitude constraints:

$$T_{\min} \leq T \leq T_{\max} \tag{11}$$

$$\begin{aligned} |\tau_\phi| &\leq \tau_{\max} \\ |\tau_\theta| &\leq \tau_{\max} \\ |\tau_\psi| &\leq \tau_{\max} \end{aligned} \tag{12}$$

$$\begin{aligned} |\phi| &\leq \phi_{\max} \\ |\theta| &\leq \theta_{\max} \end{aligned} \tag{13}$$

The implementation logs constraint-activation indicators at each time step:

- **Thrust activity:** $a_T(k) = 1$ if $T(k)$ is within a small tolerance of $T_{\min}$ or $T_{\max}$.
- **Torque activity:** $a_\tau(k) = 1$ if any $|\tau_i(k)|$ is within tolerance of $\tau_{\max}$.
- **Attitude-bound proximity:** $a_\eta(k) = 1$ if $|\phi(k)|$ or $|\theta(k)|$ approaches its bound.

These indicators define constraint-inactive versus constraint-active regimes and allow identification of regime transitions induced by feasibility geometry. Such regime-dependent behavior is consistent with perspectives from switched and hybrid systems in which qualitative response changes occur across mode boundaries [20, 21]. To explicitly address the scientific questions, two controlled experiments were designed to elicit distinct nonlinear regimes:

Experiment 1: Tight constraint regime (constraint-induced dynamics). Actuator and attitude limits are tightened (reduced T_{max}, reduced τ_{max}, and narrower ϕ_{max} and θ_{max}) to intentionally increase constraint activation. This experiment isolates how feasibility boundaries reshape control allocation and transient behavior, enabling comparison between constraint-inactive and constraint-active regimes.

Experiment 2: Aggressive maneuver regime (coupling-dominated dynamics). The reference trajectory rate is increased while maintaining the same geometric figure-eight path. This increases required lateral accelerations and amplifies translational–rotational coupling, revealing how nonlinear coupling dominates the response and pushes the system toward constraint boundaries even when constraint limits are unchanged.

Together, these experiments enable a systematic comparison of nonlinear operating regimes and transitions, supporting a system-level interpretation of nonlinear model predictive control controlled behavior as emerging from the coupling of nonlinear prediction and constrained optimization [6, 9, 19].

3 Results

The effectiveness of the proposed nonlinear model predictive control framework was evaluated through numerical simulations using a full nonlinear quadrotor model implemented in MATLAB. The controller was tested on a three-dimensional trajectory tracking task consisting of a smooth figure-eight reference motion in the horizontal plane, combined with constant altitude flight and fixed yaw. The simulation horizon was 10 s with a sampling time of 50 ms.

Figure 2, Figure 3, and Figure 4 report the time-domain tracking performance along the x, y, and z directions. In Figure 2, the quadrotor position along the x-axis closely follows the sinusoidal reference after a brief transient interval caused by the initial condition mismatch. After convergence, tracking remains bounded and stable. Figure 3 shows similarly smooth tracking along the y-axis, demonstrating that the controller manages nonlinear lateral coupling without oscillatory overshoot. Altitude regulation is shown in Figure 4, where the quadrotor maintains the reference height of 1 m with negligible steady-state offset, consistent with the vertical weighting in the objective function.

Figure 5 depicts the three-dimensional spatial trajectory compared to the desired reference path. The tracked trajectory closely overlaps the reference curve, confirming coordinated motion control in three dimensions and stable closed-loop evolution under nonlinear dynamics.

The control inputs generated by the nonlinear model predictive control optimization are shown in Figure 6 and Figure 7. The thrust command (Figure 6) exhibits an initial increase above hover to accelerate toward the moving

reference, followed by bounded periodic modulation aligned with the trajectory. Figure 7 shows smooth roll and pitch torque variations required for lateral maneuvering, while the yaw torque remains near zero due to the fixed yaw reference. The smoothness of the control inputs reflects the manipulated-variable rate penalty, and the boundedness confirms explicit enforcement of actuator constraints within the optimization loop.

To move beyond performance display and explicitly characterize nonlinear behavior, a regime indicator signal is introduced in Figure 8. The plotted binary indicators represent thrust saturation activity, torque-bound activity, and attitude-bound proximity. In the baseline case, the system operates predominantly in a constraint-inactive regime, where the optimization is governed mainly by tracking and regularization terms. Under tighter constraints or more demanding trajectories, the indicator activation increases, revealing constraint-active intervals where feasibility reshapes the optimization solution and alters the closed-loop dynamics.

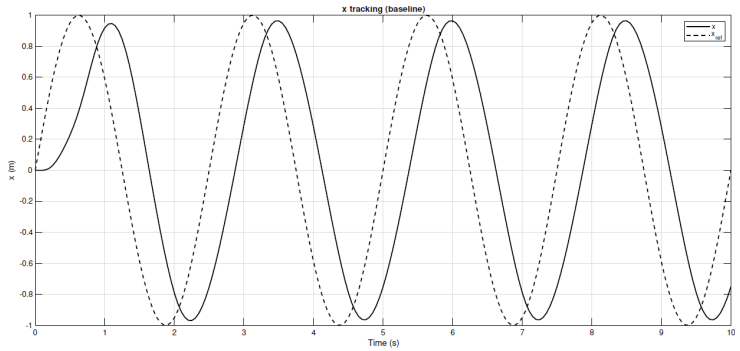

Figure 2. Time-domain tracking performance along the x-axis

Note: The solid line representing the quadrotor position controlled by the nonlinear model predictive control scheme and the dashed line denoting the reference.

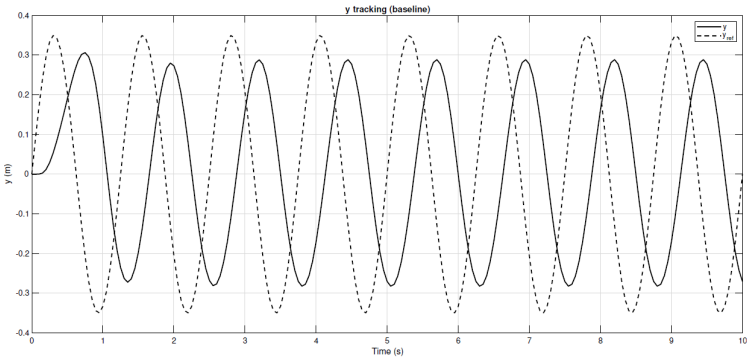

Figure 3. Time-domain tracking performance along the y-axis

Note: The nonlinear model predictive control controller closely following the figure-eight reference with smooth and bounded response.

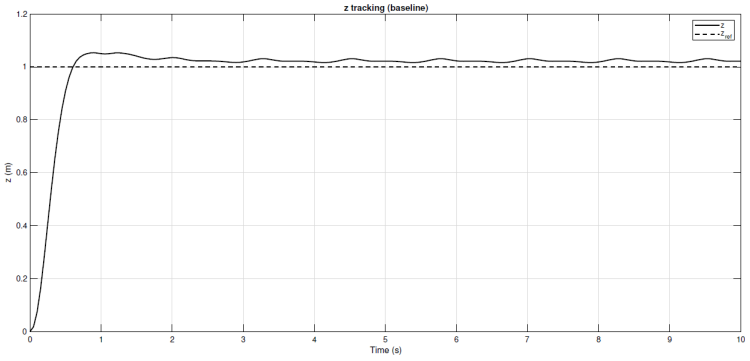

Figure 4. Altitude tracking along the z-axis

Note: The quadrotor maintaining the desired constant height of 1 m with negligible deviation.

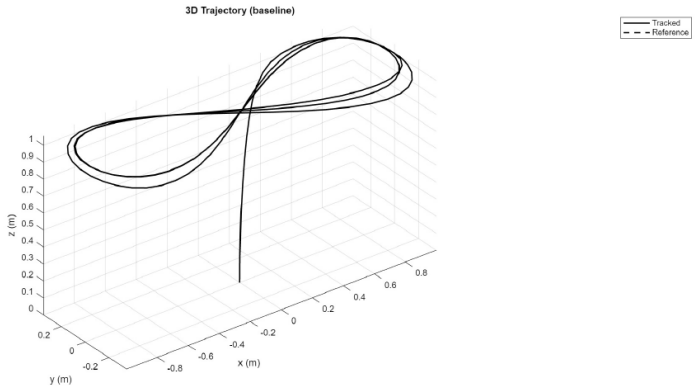

Figure 5. Three-dimensional trajectory tracking
Note: The tracked trajectory (solid) closely overlaps the reference figure-eight path (dashed), confirming accurate spatial coordination.

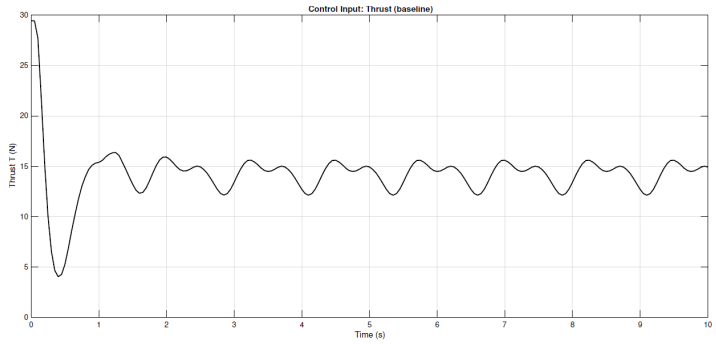

Figure 6. Total thrust command generated by the nonlinear model predictive control controller
Note: The thrust remains smooth and bounded within the imposed limits while enabling accurate tracking.

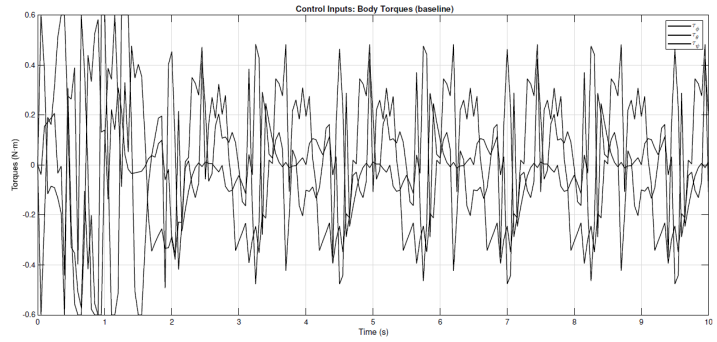

Figure 7. Body torque inputs
Note: Roll and pitch torques exhibit smooth periodic variations associated with lateral accelerations, whereas yaw torque remains near zero due to the fixed yaw reference.

Beyond nominal tracking, comparative simulations were conducted for mild versus aggressive maneuvers and for relaxed versus tight constraint boundaries. Under mild maneuvering, the response converges to a smooth quasi-periodic regime with bounded inputs. Under aggressive maneuvering, translational–rotational coupling becomes dominant, producing larger amplitude thrust modulation and roll/pitch torque variation. Under tight constraints, feasibility becomes the dominant limitation, yielding constraint-active intervals with increased tracking deviations followed by recovery once constraints deactivate. Table 1 summarizes quantitative indicators, including tracking error metrics and the percentage of time the system operates in a constraint-active regime.

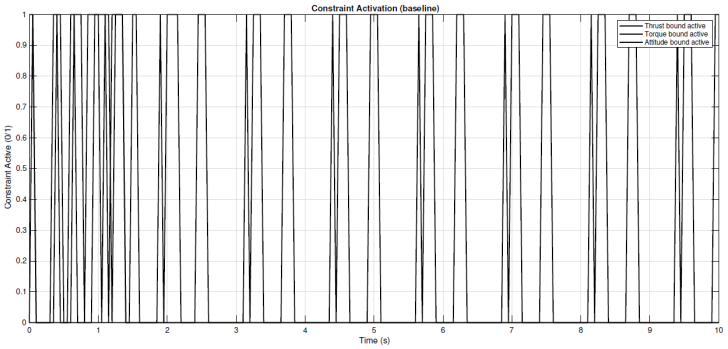

Figure 8. Constraint-activation regime indicators

Note: The binary signals indicate activation of thrust saturation, torque saturation, and attitude-bound proximity, enabling identification of constraint-inactive versus constraint-active nonlinear operating regimes.

Table 1. Quantitative behavioral comparison across maneuver and constraint settings

Case	RMSE$_x$ (m)	RMSE$_y$ (m)	RMSE$_z$ (m)	Percentage of Time (Constraint-Active)
Relaxed (constraint-inactive)	0.5170	0.3228	0.1536	0.50
Baseline (mild maneuver)	0.6136	0.3621	0.1571	35.32
Aggressive maneuver	23.5198	35.8411	28.5444	100.00
Tight constraints	1.1500	0.3023	0.2512	100.00

Note: RMSE = Root Mean Square Error.

4 Analysis of Constraint-Induced Nonlinear Regimes and Stability Structure

Although nonlinear model predictive control is often evaluated by tracking accuracy and constraint satisfaction, the closed-loop response is fundamentally governed by the interaction between nonlinear dynamics, constraint activation, and receding-horizon optimization [6, 9]. In this section, the objective is to characterize nonlinear behavior and interpret stability-relevant structure through regime identification.

In constraint-inactive regions, the controller operates in a near-linear regime around the reference trajectory, where the quadratic weights dominate the optimizer. In constraint-active regions, the feasible set reshapes the optimizer solution, producing a feasibility-limited regime with distinct transient behavior. The regime indicator in Figure 8 provides direct evidence for such transitions. Aggressive maneuvers increase coupling demand and push the system toward constraint boundaries, whereas tight constraints increase the prevalence of constraint-active operation. These effects demonstrate that nonlinear model predictive control induces a piecewise-defined closed-loop mapping where qualitative behavior changes depend on constraint activation [20–22].

5 Discussion

The results demonstrate accurate trajectory tracking with smooth thrust and torque commands while enforcing actuator and attitude constraints. Beyond performance metrics, the system-level significance of this work lies in interpreting closed-loop behavior as an emergent property of nonlinear coupling, constraint boundaries, and optimization-based feedback [6, 9, 19]. In this perspective, nonlinear model predictive control functions not only as a controller but also as a structured mechanism for revealing constraint-induced nonlinear regimes and transitions [5, 8]. Although the case study focuses on a quadrotor unmanned aerial vehicle, the observed regime-based behavior generalizes to other constrained nonlinear dynamical systems such as robotic manipulators under torque bounds, legged robots under contact constraints, and biomechatronic devices with saturation and safety limits. In these systems, constraints do not merely clip inputs; rather, they reshape feasible control authority and can alter qualitative closed-loop response. Thus, nonlinear model predictive control can be interpreted as a general tool for exploring how nonlinear coupling and feasibility geometry shape motion behaviors across intelligent dynamical systems [6].

From a nonlinear science viewpoint, constraint activation introduces regime-dependent structure resembling switching behavior between constraint-inactive and constraint-active modes [20]. While plant dynamics remain continuous, the closed-loop mapping becomes piecewise defined by active constraints, producing hybrid-like behavior induced by the optimizer [21, 22]. Under mild maneuvers, the response converges to a quasi-periodic tracking regime, whereas aggressive maneuvers amplify coupling-dominated behavior and tight constraints yield feasibility

limited dynamics. These observations support the interpretation that closed-loop properties emerge from the competition between coupling-induced demand and constraint-limited authority, mediated through receding-horizon optimization. Practically, the results also highlight that nonlinear model predictive control tuning parameters such as horizon lengths and weight selection shape regime boundaries. Larger tracking weights increase actuation demand and may push operation toward constraint activation, whereas stronger control-rate penalties mitigate abrupt transitions. Prediction horizon length influences the ability to anticipate curvature and constraint engagement, affecting smoothness and feasibility margins [5]. Future work may extend this analysis by incorporating disturbances, parameter uncertainty, estimation errors, and computational constraints that influence real-time feasibility and robustness [19].

6 Conclusions

This study proposed a nonlinear model predictive control framework for quadrotor unmanned aerial vehicle trajectory tracking based on a physics-driven rigid-body nonlinear model and a receding-horizon constrained optimization scheme. Beyond demonstrating accurate three-dimensional tracking with smooth thrust and torque commands, the study emphasized a system-level interpretation of nonlinear closed-loop dynamics shaped by constraint activation and translational–rotational coupling. Comparative simulations under different maneuver intensities and constraint boundaries revealed distinct constraint-inactive and constraint-active operating regimes, where aggressive trajectories amplify coupling-dominated behavior and tightened feasibility limits induce constraint-driven dynamics that dominate transient response. Overall, these findings confirm nonlinear model predictive control as both an effective control strategy for quadrotor tracking and a structured tool for analyzing nonlinear behavior and regime transitions in constrained intelligent dynamical systems.

Author Contributions

Conceptualization, M.M. and M.K.; methodology, M.M. and M.K.; software, M.M. and M.K.; validation, M.M. and M.K.; formal analysis, M.M. and M.K.; investigation, M.M. and M.K.; resources, M.M. and M.K.; writing—original draft preparation, M.M. and M.K.; writing—review and editing, M.M. and M.K.; visualization, M.M. and M.K.; supervision, M.M. and M.K. All authors have read and agreed to the published version of the manuscript.

Data Availability

The data used to support the research findings are available from the corresponding author upon request.

Acknowledgements

The authors acknowledge the Sakarya University of Applied Sciences (https://subu.edu.tr/) for the technical support provided to publish the present manuscript.

Conflicts of Interest

The authors declare no conflicts of interest.

References

[1] S. N. Ghazbi, Y. Aghli, M. Alimohammadi, and A. A. Akbari, "Quadrotors unmanned aerial vehicles: A review," *Int. J. Smart Sens. Intell. Syst.*, vol. 9, no. 1, pp. 309–333, 2016. https://doi.org/10.21307/ijssis-2017-872

[2] M. Idrissi, M. Salami, and F. Annaz, "A review of quadrotor unmanned aerial vehicles: Applications, architectural design and control algorithms," *J. Intell. Robot. Syst.*, vol. 104, no. 2, p. 22, 2022. https://doi.org/10.1007/s10846-021-01527-7

[3] Q. A. Mumuni, A. I. Olayiwola-Mumuni, and A. A. Yussouff, "The advent of the proportional integral derivative controller: A review," *J. Adv. Eng. Technol.*, vol. 2, no. 1, pp. 5–22, 2023.

[4] E. A. Gedefaw, N. B. Abera, and C. M. Abdissa, "A review of modeling and control techniques for unmanned aerial vehicles," *Eng. Rep.*, vol. 7, no. 6, p. e70215, 2025. https://doi.org/10.1002/eng2.70215

[5] M. Schwenzer, M. Ay, T. Bergs, and D. Abel, "Review on model predictive control: An engineering perspective," *Int. J. Adv. Manuf. Technol.*, vol. 117, no. 5-6, pp. 1327–1349, 2021. https://doi.org/10.1007/s00170-021-07682-3

[6] J. B. Rawlings, D. Q. Mayne, and M. Diehl, *Model Predictive Control: Theory, Computation, and Design*. Madison, WI: Nob Hill Publishing, 2020.

[7] M. Bangura and R. Mahony, "Real-time model predictive control for quadrotors," *IFAC Proc. Vol.*, vol. 47, no. 3, pp. 11 773–11 780, 2014. https://doi.org/10.3182/20140824-6-ZA-1003.00203

[8] J. Berberich and F. Allgöwer, "An overview of systems-theoretic guarantees in data-driven model predictive control," *Annu. Rev. Control Robot. Auton. Syst.*, vol. 8, no. 1, pp. 77–100, 2025. https://doi.org/10.1146/annurev-control-030323-024328

[9] D. Q. Mayne, J. B. Rawlings, C. V. Rao, and P. O. M. Scokaert, "Constrained model predictive control: Stability and optimality," *Automatica*, vol. 36, no. 6, pp. 789–814, 2000. https://doi.org/10.1016/S0005-1098(99)00214-9

[10] J. C. Pereira, V. J. S. Leite, and G. V. Raffo, "Nonlinear model predictive control on SE(3) for quadrotor aggressive maneuvers," *J. Intell. Robot. Syst.*, vol. 101, no. 3, p. 62, 2021. https://doi.org/10.1007/s10846-021-01310-8

[11] D. Wang, Q. Pan, Y. Shi, J. Hu, and C. Zhao, "Efficient nonlinear model predictive control for quadrotor trajectory tracking: Algorithms and experiment," *IEEE Trans. Cybern.*, vol. 51, no. 10, pp. 5057–5068, 2021. https://doi.org/10.1109/TCYB.2020.3043361

[12] Z. Wang, X. Li, Y. Zhang, and P. Huang, "Localization, planning, and control of a UAV for rapid complete coverage bridge inspection in large-scale intermittent GPS environments," *IEEE Trans. Control Syst. Technol.*, vol. 32, no. 4, pp. 1357–1369, 2024. https://doi.org/10.1109/TCST.2024.3366695

[13] B. Jiang, B. Li, W. Zhou, L. Y. Lo, C. K. Chen, and C. Y. Wen, "Neural network based model predictive control for a quadrotor UAV," *Aerospace*, vol. 9, no. 8, p. 460, 2022. https://doi.org/10.3390/aerospace9080460

[14] E. Wang, "A summary of the application of mathematics in the design of quadrotor UAV," *Front. Sci. Eng.*, vol. 5, no. 10, pp. 77–84, 2025. https://doi.org/10.54691/rnazjw69

[15] B. K. Singh and A. Kumar, "Model predictive control using LPV approach for trajectory tracking of quadrotor UAV with external disturbances," *Aircr. Eng. Aerosp. Technol.*, vol. 95, no. 4, pp. 607–618, 2023. https://doi.org/10.1108/AEAT-12-2021-0368

[16] Z. Xu, L. Fan, W. Qiu, G. Wen, and Y. He, "A robust disturbance-rejection controller using model predictive control for quadrotor UAV in tracking aggressive trajectory," *Drones*, vol. 7, no. 9, p. 557, 2023. https://doi.org/10.3390/drones7090557

[17] X. Lan, L. Gong, L. Zheng, S. Liu, and W. Xu, "Anti-swing strategy of a quadrotor with suspended payload based on model predictive control," in *2023 9th International Conference on Control Science and Systems Engineering (ICCSSE)*, Shenzhen, China, 2023, pp. 20–25. https://doi.org/10.1109/ICCSSE59359.2023.10245849

[18] D. Du, M. Chang, L. Tang, H. Zou, C. Tang, and J. Bai, "Trajectory planning and control design for aerial autonomous recovery of a quadrotor," *Drones*, vol. 7, no. 11, p. 648, 2023. https://doi.org/10.3390/drones7110648

[19] M. Diehl, H. G. Bock, and J. P. Schlöder, "Real-time optimization and nonlinear model predictive control of processes governed by differential-algebraic equations," *J. Process Control*, vol. 12, no. 4, pp. 577–585, 2002. https://doi.org/10.1016/S0959-1524(01)00023-3

[20] D. Liberzon, *Switching in Systems and Control*. Boston, MA: Birkhäuser, 2003.

[21] A. R. Teel, *Hybrid Dynamical Systems: Modeling, Stability, and Robustness*. Princeton University Press, 2012.

[22] M. di Bernardo Laurea, A. R. Champneys, C. J. Budd, and P. Kowalczyk, *Piecewise-Smooth Dynamical Systems: Theory and Applications*. Springer Science & Business Media, 2008.